Research Article

Simulation and Experimental Studies on Sustainable Process Optimization of CO_2 Adsorption Using Zeolite 5A Pellet

Boonthita Wongchalerm, Thanaporn Arunchai, Thanayut Khamkenbong, Supawon Sangsuradet and Anurak Pitiraksakul
Department of Chemical Engineering, Faculty of Engineering, King Mongkut's University of Technology North Bangkok, Bangkok, Thailand

Patcharin Worathanakul*
Department of Chemical Engineering, Faculty of Engineering, King Mongkut's University of Technology North Bangkok, Bangkok, Thailand
Center of Eco-Materials and Cleaner Technology (CECT), King Mongkut's University of Technology North Bangkok, Bangkok, Thailand

* Corresponding author. E-mail: patcharin.w@eng.kmutnb.ac.th DOI: 10.14416/j.asep.2022.04.004
Received: 14 Novembet 2021; Revised: 8 December 2021; Accepted: 10 February 2022; Published online: 20 April 2022

Abstract
This study focused on a quantitative study of the CO_2 adsorption dynamic within the adsorbent particle. It could drive and improve ideal pore characteristics and the adsorption process efficiency. The parameters operating conditions for the CO_2 adsorption process of zeolite 5A pellet were studied using Aspen Adsorption. The effects of compression force (200–400 MPa), compression time (5–15 min), and addition of bentonite binder (0–15% wt. of bentonite binder) for zeolite 5A pelletization and temperature for CO_2 adsorption ranging from 298–373 K were studied. There was an error from the simulation of approximately 0.34–10.62% compared to the experimental results. The results showed that the interparticle voidage was reduced, and the appropriate mass transfer was required for good CO_2 adsorption capacity. Reduction of interparticle voidage is achieved using a small compression force, a short compression duration, and a small bentonite binder, all of which significantly increase CO_2 adsorption capacity. The mass transfer must be within the optimum range because it will decrease the contact time between the zeolite surface and the CO_2 molecules. The CO_2 adsorption increases with the gas phase temperature decrease. The result showed that the maximum CO_2 adsorption by zeolite 5A was 7.078 mmol CO_2/g with 0 wt% bentonite binder, 200 MPa, and 5 min at 298 K, 1 atm pressure.

Keywords: Zeolite 5A, Pellet, Carbon dioxide, Gas adsorption, Adsorption simulation

1 Introduction

Nowadays, the emission of CO_2 from various sources, such as combustion activities and industrial processes, has continuously increased atmospheric CO_2 levels and significantly contributed to global warming, as CO_2 is one of the main greenhouse gases. There are several solutions to reduce the carbon dioxide emissions. The most popular method is adsorption, adsorption is the adhesion of atoms, ions or molecules from a gas, liquid, or dissolved solid to a surface. At present, there are many studies involved in carbon dioxide adsorption. In previous works, activated carbon, zeolite, and silica-based are usually used as adsorbents [1]–[5].

Zeolite is a material with unique physical and chemical properties. Zeolites 5A is a microporous material suitable for the adsorption of various sizes of gas molecules. Moreover, its surfaces are formed with negatively charged oxides for gas adsorption. Many studies have been done on the CO_2 adsorption of

Zeolite 5A. The commercial zeolite 5A granules with 1.6–3 mm in diameter had a CO_2 adsorption capacity of 3.75 to 4.50 mmol of CO_2/g of zeolite at 90–100 and 273–298 K, respectively [6], [7]. In addition, zeolite pellets were also used in CO_2 adsorption with 1.35–3.32 mm in pellet diameter had a CO_2 adsorption capacity at 273–423 K, which varied from 1.2 to 3.3 mmol of CO_2 /g of zeolite [8], [9]. Based on the literature review, it was found that the CO_2 adsorption capacity on the zeolites 5A was enhanced when the partial CO_2 pressure increased and was decreased with an increase in temperature.

Researchers have previously investigated the pressure impact on pellet properties during the pelletization process. Surface area and pore volume were observed to decrease as the pressure pelleted increased. It led to a reduction in CO_2 adsorption capacity, poor CO_2 internal mass transfer, and slow CO_2 diffusion through porous materials. Due to pore blocking and collapse of pore structures under the press, pelletization resulted in slightly decreased adsorption compared to powder adsorbent [10]–[13].

Previous simulations were done in the Aspen Adsorption research having the CO_2 removal method of coal and gas-fired power stations. The parameters and other operating conditions for the Aspen Plus rate-based model were chosen to achieve a CO_2 removal with 85 percent. As the concentration of monoethanolamine (MEA) and the temperature increased, the removal efficiency also increased. As the MEA solvent loading was increased, the effectiveness of the removal process decreased. To understand the model behavior, the liquid and vapor phase temperature profiles, and CO_2 loading in the absorber were studied [14]. Boonchuay and co-workers carried out a recent studyand showed that Zeolite 13X could adsorb CO_2 more than zeolite 5A because the polarity of Na^+ in zeolite 13X is higher than the polarity of Ca^{2+} in zeolite 5A with CO_2 molecules [15]. The physical properties and diffusion steps influenced CO_2 adsorption capabilities. Hesam *et al.* [16] showed that the pressure swing adsorption (PSA) technique was used to remove carbon dioxide from a carbon dioxide/methane combination. These findings revealed that Zeolite 13X had a higher CO_2 adsorption capacity than activated carbon and UTSA-16 MOF. In the PSA cycle, zeolite 13X had the best performance and could produce a methane product with a purity of 99.99 mole percent.

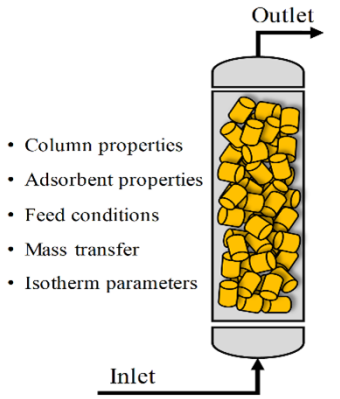

Figure 1: Flowsheet adsorption process in Aspen Adsorption.

Physical processes from simulations could produce the calculation results, but they could not generate the phenomenon, while experiments could provide new knowledge. The literature review and previous work [17]–[19] were found that most of them were studied based on experiments. Therefore, the motivation behind the current research is to identify the suitable conditions of CO_2 adsorption on zeolite 5A pellet by Aspen Adsorption simulation program simulation and comparison with experiments. The zeolite pellets had different shaping conditions, including 200–400 MPa compression forces, 5–15 min compression times, and 0–15% wt. of bentonite. The research should significantly help to reduce the need for extensive experiments and simulations.

2 Methods

2.1 *CO_2 adsorption experiment*

Commercially zeolite 5A powder for the pelletization process was purchased from Thai Silicate Chemicals Co., Ltd., Thailand as shown in Figure 1. The bentonite clay used, as a binder of zeolite pellets was purchased from NIC Interchem Co., Ltd., Thailand. The zeolite powder was mixed with water and the appropriate amount of bentonite binder. Pelletization was performed using a hydraulic press machine with a force of 200–400 kPa for 5, 10, and 15 min. The zeolite pellet was calcined after drying. The zeolite pellets that resulted were cylindrical in shape, with a diameter of 0.5 cm and a height of 0.5 cm (Figure 2).

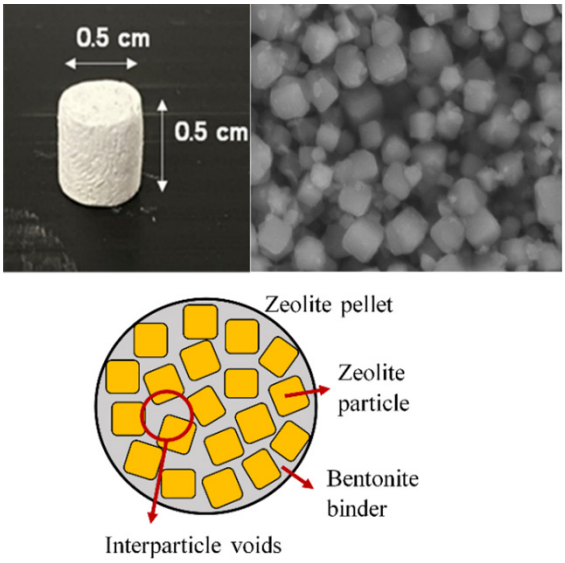

Figure 2: Zeolite 5A pellet adsorbent.

B0P2T5, B0P3T5, B0P4T5, B5P3T5, B9P3T5, B15P3T5, B5P3T10, and B5P3T15 were the names given to the zeolite pellet samples based on their pelletized condition. The number following each symbol denoted the weight percent of bentonite binder, the compression force, and the compression times. When B, was denoted the weight percent of bentonite binder, P was denoted the compression force, and T was denoted the compression time. Nitrogen adsorption isotherm measurements were used to calculate the specific surface area. A Bell model BELSORP-mini equipment was used to investigate the surface area and porosity analyzer. The zeolite pellet sample was prepared by taking the entire pellet without breaking it.

The adsorption column was packed with 1 g zeolite 5A pellets. In a furnace attached to a CO_2 analyzer (Handheld carbon dioxide meter, GM 70), the adsorption column was at atmospheric pressure, 298 K, a CO_2 flow rate of 2 L/h, and the zeolite pellet of CO_2 adsorption were investigated.

The CO_2 adsorption capacity was defined in Equation (1). Where qe is the equilibrium adsorption capacity, C0 and C are the concentrations initial and equilibrium of CO_2, respectively, v is CO_2 flow rate; MW is the molecular weight of CO_2, W is the weight of zeolite pellet, and t is time. The data were collected every 30 s for the first 20 min. After that, it was collected data every 5 min.

$$q_e = \left(\frac{C_0 - C}{W}\right) \times \frac{V_t}{M_w} \quad (1)$$

2.2 *Adsorption modelling*

A process simulator, namely Aspen Adsorption, was used to simulate the adsorption of CO_2. Aspen Adsorption is a useful flowsheet simulator for the analysis, design, simulation, and optimization of various gas and liquid adsorption processes at both the industrial and the laboratory scales. This software application could simulate ion exchange, liquid phase adsorption, and gas phase adsorption processes that simplify involved both adsorption and reaction of gas adsorption systems [20]. It was an equation-oriented simulator and provided numerous data libraries that made designing and configuring the simple adsorption flowsheets [21].

An adsorption model based on the following assumptions was formulated in this simulator. The mathematical model equations together with the correlation used for the estimation of mass and heat transfer parameters. Assumptions for physical adsorption process were as follow [22].

Firstly, material balance is convection only. Secondly, momentum balance is Ergun's equation. (Ergun equation for flow is used in a packed bed). Thirdly, energy balance is non-isothermal with no conduction (Non-isothermal operation of adsorption process has occurred in a packed bed). It is also commonly assumed that the heat transfer resistance between the gas and the solid phases is negligible and it reaches thermal equilibrium instantaneously. Fourthly, mass transfer coefficient is constant. The mass transfer mechanism is controlled by diffusion through macropores with contributions from Knudsen and molecular diffusion mechanisms. Fifthly, the kinetic model has Lumped resistance. Multiple resistances in series are included in external film resistance, surface resistance, diffusion in macropores, and diffusion in micropores. Lastly, the specific heat capacity of adsorbent is constant. Specific heat capacity of dry adsorbents is constant.The essential inputs required for starting the calculations were the physical properties of the column and adsorbents, feed conditions, mass transfer, and isotherm parameters, as shown in Figure 1.

Table 1: Physical properties of Zeolite 5A pellet

Zeolite	Condition of Pelletization: Binder (wt%), Compression Force(kPa), Compression Time (min)	Density (kg/m^3)	Specific Surface Area (m^2/g)	Pore Volume (cm^3/g)	Interparticle Voidage	Intraparticle Voidage	Heat of Adsorption CO_2 (kJ/mol)
B0P2T5	0, 200, 5	1294.27	353.43	0.2523	0.156	0.045	–86.45
B0P3T5	0, 300, 5	1324.84	354.46	0.2541	0.157	0.047	–107.64
B0P4T5	0, 400, 5	1593.52	365.22	0.2600	0.334	0.045	–256.64
B5P3T5	5, 300, 5	1630.57	303.40	0.2162	0.307	0.061	–348.68
B9P3T5	9, 300, 5	1719.75	269.49	0.1920	0.281	0.041	–87.31
B15P3T5	15, 300, 5	1823.07	306.64	0.2174	0.333	0.045	–25.20
B5P3T10	5, 300, 10	1640.76	330.80	0.2331	0.246	0.052	–78.95
B5P3T15	5, 300, 15	1898.09	275.17	0.1961	0.483	0.034	–88.25

Some of these inputs were fixed while, others varied with operating conditions. For example, the porosity of the adsorbent was fixed during the study, while mass transfer parameters changed with operating conditions.

Data for program modeling included the physical properties of the adsorbent column, the adsorbent, and the conditions of operation. The adsorbent material was zeolite 5A, and CO_2 was adsorbates for this research. The adsorbents' physical properties and the packing column's are shown in Tables 1 and 2. Therefore, the main objectives of this research were to study the factors affecting CO_2 adsorption and on zeolite 5A at temperatures ranging from 298 to 373 K with the program Aspen Adsorption® simulation program (version V11, Aspen Technology, Inc., Bedford, MA, USA).

2.3 *The properties of zeolite 5A pellet adsorbent*

Zeolites are three-dimensional aluminosilicates: A periodic array of SiO_4/AlO_4 composed of Si and Al tetrahedra linked through bridging oxygen atoms give rise to a periodic distribution of pores and cavities of molecular dimensions. This microporous adsorbent represents a breakthrough in adsorption due to its uniform pore structure (4 to 6 Å), comprehensive topology, high thermal, high hydrothermal, and high chemical stability. There are different criteria, including pore aperture, the shape of pores, dimensionality of the channel, and channel connections according to which the structure of zeolites can be classified. Zeolites can be found in nature or can be synthesized. The pore structures are controlled for synthesized zeolites by replacing negatively charged alumina with cations. Zeolites 5A is one group of zeolite having an LTA-type structure with the ideal unit cell equivalent to 8 α-cages and 24 cubic and the chemical formula $Ca_4,5Na_3[(AlO_2)12(SiO_2)_{12}]\cdot zH_2O$.

The zeolite pellet was cylindrical with 0.5 cm diameter and 0.5 cm height, as shown in Figure 2. The zeolite pellet samples were named according to pelletized conditions B0P2T5, B0P3T5, B0P4T5, B5P3T5, B9P3T5, B15P3T5, B5P3T10, and B5P3T15 were denoted B referring to wt% of bentonite binder, P represents the compression force, and T is compression time.

The zeolite 5A pellet was used to study the influence on the CO_2 adsorption process. The physical properties of the adsorbents are presented in Table 1. It showed that the increasing bentonite content led to a reduction in the surface area.

The CO_2 adsorption process with 2 L of CO_2/h feeding was introduced into the packed bed reactor at the bottom of the adsorber at 298, 333, and 373 K with the atmospheric pressure. The CO_2 went direct contact through the zeolite 5A pellet adsorbent in the packed bed reactor. The characteristics of the column used are shown in Table 2.

Table 2: Parameters of adsorption process

Column Characteristics	
Height of adsorbent layer, H_b (mm)	120
Internal diameter of adsorbent layer, D_b (mm)	20
Adsorbent particle radius, R_p (cm)	0.25
Adsorbent shape factor	1.0

2.4 *Mass transfer model*

The mass transport models used to formulate the equations for the adsorbent bed and the adsorbent particles were essential parts of the overall model. The diffusion

coefficient could be generally obtained from the experiment. However, some data may be hard to reach because of the limitation of experimental conditions. It may be necessary to use a calculation method from the quasi-theoretical equation or the empirical equation.

2.4.1 Gas-phase binary diffusion coefficient

The kinetic theory was used to describe the gravity and the intermolecular force of mixed gas using the Lennard-Jones theory to evaluate intermolecular forces by the diffusion coefficient of the mixed gas. The assumptions were based on nonpolar molecules and no reaction. It could be calculated from Equation (2) [23].

$$D_{AA} = \frac{2T^{3/2}}{3\pi^{3/2}\sigma_A^2 P}\left(\frac{K^3 N}{M_A}\right)^{1/2} \quad (2)$$

When D_{AA} is the diffusion coefficient of A (cm^2/s), T is the temperature (K), P is the pressure (atm), MA is the molecular weight of substance A, σ_A is the collision diameter of the substance A (Å), and K is Boltzman constant.

2.4.2 Mass transfer coefficient

The mass transfer constant within the adsorbent was determined from the theory of pore diffusion, in which the diffusion of the adsorbed molecular diffusion was used. Knudsen diffusion is determined by diffusion of the adsorbed molecules through porosity of the adsorbent. If the diameter of the pore is smaller than the mean distance of movement of the adsorbed molecule in each collision (Mean free path), the adsorbed molecule collides with the pore surface area of more absorbent material [24]. The CO_2 molecule size is 3.34 Å, near the pore size of zeolite 5A. Hence Knudsen diffusion is a decent candidate, as shown in Equation (3).

$$D_{KA} = 4850\ d_{pore}\sqrt{\frac{T}{M_A}} \quad (3)$$

When D_{KA} is the Knudsen diffusion coefficient of substance A (cm^2/s), D_{pore} is the substance's diameter (Å). The diffusion constant within porosity was determined in Equation (4).

$$\frac{1}{D_{pi}} = \tau\left[\frac{1}{D_{KA}} + \frac{1}{D_{AB}}\right] \quad (4)$$

When D_{pi} is diffusion coefficient (cm^2/s), and τ is winding value within the porous material.

The tortuosity of porous media (τ) can be determined from Equation (5) [25].

$$\tau = \left[1-\alpha(1-\varepsilon_p)\right]^{-1} \quad (5)$$

Where α = 0.75 and transfer constant in sorbent material can be calculated from Equation (6) [26].

$$k_i = \frac{15\varepsilon_p D_{pi}}{r_p^2} \quad (6)$$

Where k_i is the mass transfer constant (1/s). And r_p is the radius of the sorbent material (cm)

2.5 *Adsorption isotherm*

Adsorption isotherm describes the relationship between the balanced concentration and the number of adsorbates that are adsorbent at constant temperature for adsorption of the adipose. The dissolution on the hard surface is the relationship between the adsorption volume and the concentration of the solution. Equilibrium at any temperature [27].

Langmuir isotherm was primarily designed and developed to explain gas-solid phase adsorption. It is now also used to compare and measure the adsorptive capacity of different adsorbents [27]. The Langmuir isotherm balances the relative rates of adsorption and desorption to account for surface coverage (dynamic equilibrium). Adsorption is proportional to the fraction of the surface of the adsorbent that is open while desorption is proportional to the fraction of the adsorbent surface that is covered [28].

2.5.1 Langmuir isotherm

The Langmuir adsorption model explains adsorption by assuming an adsorbate behaves as an ideal gas at isothermal conditions. The Langmuir equilibrium equation can be expressed as Equation (7) [28]–[35].

$$q = \frac{q_m b C_e}{1 + b C_e} \quad (7)$$

The Langmuir equation can be written as a linear Equation (8).

$$\frac{1}{q} = \frac{1}{q_m} + \frac{1}{bq_mC_e} \quad (8)$$

When q is the amount of adsorbed on the sorbent surface area per the sorbent volume (mg/g), q_m is the maximum adsorption capacity (mg/g), C_e is the concentration of the absorbed substance at the equilibrium point (mg/g), And b is the Langmuir adsorption constant (L/mg) [20].

3 Results and Discussion

3.1 *Effect of bentonite clay on CO_2 adsorption*

The chemical formula of bentonite is varied depending on the dominating chemical element in the clay. For example, sodium bentonite has the chemical formula of $Al_2H_2Na_2O_{13}Si_4$. The Na^+ content of zeolite is like that of bentonite, and bentonite improves the strength of zeolite pellets. The quantity of bentonite binder (0–15 wt%) was required to find the suitable zeolite 5A pellet. The properties of zeolite 5A pellets are shown in Table 1. The CO_2 adsorption of the zeolite pellet was tested and simulated at atmospheric pressure, 333 K, and 2 L/h CO_2 flow rate. The adsorption capacity as a function of time is present in Figure 3. Under the same adsorption condition, binderless zeolite 5A pellets showed higher CO_2 adsorption capacities than zeolite 5A pellets with bentonite clay. It was observed that the CO_2 adsorption capacity decreased with increasing content of bentonite clay [8], [35]–[38] because increasing the content of bentonite clay led to decreasing pore volume of zeolite 5A pellet. It was due to bentonite adhered to an external surface of 5A zeolite particle and provided sufficient mechanical strength to resist attrition loss for most commercial applications. Therefore, it was difficult for the CO_2 molecules to reach the active site of adsorbents from Table 1. The interparticle, voidage of B0P3T5 was the lowest, which the zeolite particles within the pellet were very close (less interparticle) due to the absence of bentonite binder interference as shown in Figure 1. This allows the zeolite pellet without binder to have a greater attraction force between the zeolite surface and the CO_2 molecules, resulting in high adsorption capacity. In addition, the error of simulation results with the experiment was about 0.88–2.05% [39].

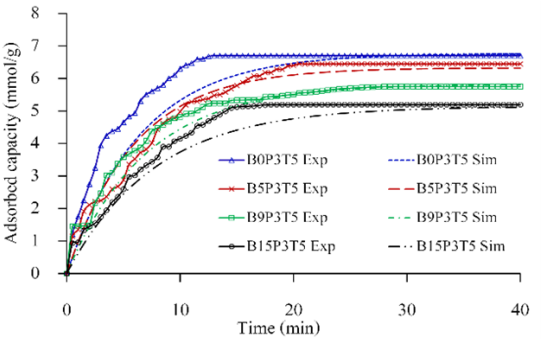

Figure 3: CO_2 adsorption capacity on different bentonite clay content.

Moreover, earlier studies on bentonite to CO_2 adsorption indicated that the CO_2 adsorption capacity was varied ranging of 0.11–0.32 mmol/g at 298–318 K and 1 atm [40]–[42]. The low adsorption capacity was observed because the structure of bentonite was composed of H_2O and cations. These molecules were implicated at high relative humidity, preventing CO_2 molecules from passing through the interlayer gap. Furthermore, the CO_2 adsorption capacity of zeolite 5A powder was 3.8 mmol/g at 298 K and 1 atm. When bentonite was added to form zeolite pellets, the pressure drop in the column was reduced. The zeolite pellets were easy to regenerate and store. However, the CO_2 adsorption efficiency of zeolites with binder was slightly lower than that of zeolites without binder.

3.2 *Effect of compression force on CO_2 adsorption*

The CO_2 adsorption of the zeolite pellets, which were formed with compression force at 200, 300, and 400 MPa, was tested and simulated under atmospheric pressure, 333 K, as shown in Figure 4. The result showed that pelletized zeolite, pelleted at 200 MPa has the highest adsorption capacity for CO_2. When compression force, However, zeolite pellet increased, the surface area also increased. Zeolite 5A particle was compressed to break into small pieces, which led to the decreased pore volume of zeolite pellets. Therefore, CO_2 molecules could not diffuse to the pore of the zeolite pellet [43]. Tables 2 and 3. showed interparticle voidage and mass transfer of zeolite pellet. It was found that B0P4T5 with the high compression force in the shaping process had the most interparticle

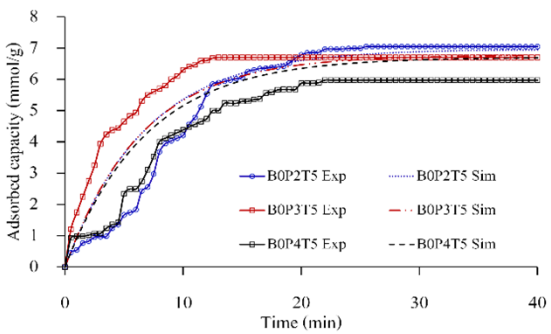

Figure 4: CO_2 adsorption capacity on different compression force.

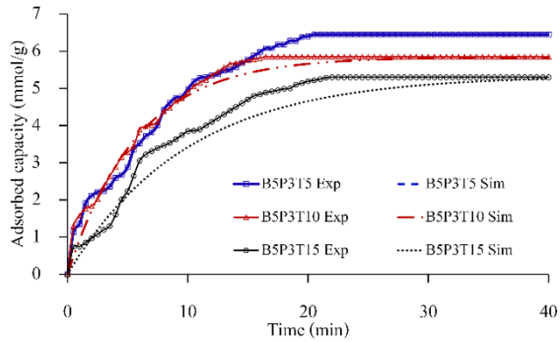

Figure 5: CO_2 adsorption capacity on different compression time.

voidage. Because the zeolite particle was broken into small pieces, there were more voids inside the zeolite pellet. While the mass transfer value of B0P4T5 was the lowest because of over-compression forces making the particles being too close together. The internal cavities may not be sufficiently moved into the pores for CO_2 molecules thus CO_2 adsorption capacity was minimized.

Table 3: Density and mass transfer coefficient for experimental

Zeolite Pellets	Mass Transfer Coefficient (k_i) × 10^{-3} (1/s)		
	298 K	333 K	373 K
B0P2T5	2.35	2.49	2.63
B0P3T5	2.47	2.61	2.76
B0P4T5	2.33	2.46	2.61
B5P3T5	2.54	2.85	2.91
B9P3T5	2.08	2.20	2.33
B15P3T5	2.31	2.44	2.58
B5P3T10	2.69	2.84	3.01
B5P3T15	1.71	1.81	1.91

The conflicting results revealed that as the compression force increased, the surface area of the pellets increased while CO_2 adsorption decreased. The zeolite 5A particle was compressed to break into small pieces, resulting in a smaller zeolite 5A particle and an increase in the density of the zeolite 5A pellet from 1294.27 to 1593.52 kg/m^3. As a result, getting CO_2 molecules to reach the zeolite particles was harsh. At 400 kPa compression forces, limitation of mass transfer resulted in CO_2 adsorption efficiency reduced.

3.3 *Effect of compression time on CO_2 adsorption*

The zeolite pellet with bentonite binder 5 wt% was varied compression time at 5, 10, and 15 min and tested CO_2 adsorption under atmospheric pressure and 333 K as shown in Figure 5. Under the same adsorption condition, zeolite was pelletized at a shorter compression time showed higher adsorption capacity for CO_2 than for which longer compression time. It was observed that the CO_2 adsorption capacity decreased with increasing compression time. This was due to increasing compressive time led to decreasing surface area and pore volume. Therefore, the contact area between zeolite and CO_2 molecule was decreased. Excessive and prolonged compression could cause permanent structural changes of the zeolite and a reduction of adsorption efficiency. In addition, zeolite pellets' compression time for 15 min showed the lowest mass transfer, which was consistent with the results that the pore volume of zeolite pellet was reduced, it made more difficult of mass transfer of CO_2 molecules.

The density of the zeolite pellet was increased by 1630.57, 1640.76, and 1898.09 kg/m^3 for compression periods of 5, 10, and 15 min, respectively. Furthermore, neither the BET surface area nor the CO_2 adsorption capacity measurements followed a theoretical pattern. Compared to 5 min, the BET surface area was considerably lowed, and the CO_2 adsorption capacity decreased after 15 min compression time as shown in Figure 5. It was affected by a decrease in the amount of active sorbent and blocked pores [34], [44].

3.4 *Effect of temperature on CO_2 adsorption*

The adsorption temperature is an important parameter to measure the kinetics of an adsorbent to evaluate its suitability for the adsorption application required. The

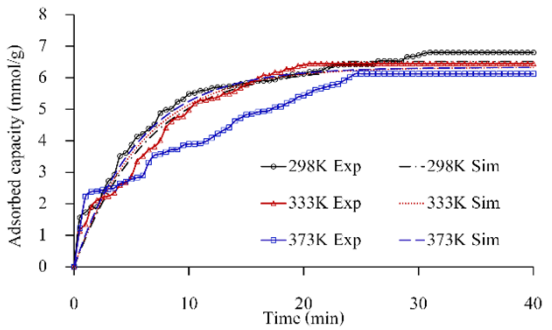

Figure 6: CO_2 adsorption capacity on different temperature.

CO_2 adsorption kinetics of zeolite pellets are shown in Table 3. At a given temperature, the mass transfer coefficient increased with increasing temperature. It was indicated that increasing temperature allowed gaseous molecules to diffuse at a greater rate, but it reduced the chance for the CO_2 to be restrained or trapped by fixed energy adsorption sites on the zeolite 5A adsorbent surface. The adsorbed capacity along the axial direction of adsorption time was at adsorption temperatures 298, 333, and 373 K, as shown in Figure 6. CO_2 was adsorbed quickly on the zeolite 5A adsorbent surface at the initial stage of the adsorption process, then the rate became slower with time, and it was reached adsorption equilibrium. It was observed that the CO_2 adsorption processes at the high temperature reached faster than at the low temperature [45], [46].

The adsorbed capacity of CO_2 was increased with decreasing temperature. It was indicated that adsorption purification was improved as we know that adsorption is an exothermic process. The more intense the adsorption, the heat is more released [28].

4 Conclusions

Experiments could be conducted to test fundamental hypotheses, which are impossible to evaluate with computer simulations. A simulation clearly could not be used to test fundamental hypotheses, because the outcome of simulation is simply determined by the hypothesis upon the simulation. The Aspen Adsorption was developed for the adsorption process to help for some experiment data reduction. The appropriated model was selected for getting mass transfer and isotherm parameters in the adsorber. It was found that there was an error of about 0.34–10.62% when compared to the experimental results. The impact of pelletization on CO_2 adsorption of zeolite 5A pellets was simulated under 200, 300, and 400 kPa pressure, compression times at 5, 10, and 15 min, 0, 5, 9, and 15 wt% of bentonite binder at 298, 333, and 373 K temperature. According to IUPAC the CO_2 adsorption isotherm was obtained, followed by a type-I isotherm classification, representing a monolayer adsorption mechanism.

The effect of content of bentonite clay, compression force, compression time, and temperature on CO_2 adsorption were carried out. The mass transfer, interparticle voidage, and intraparticle voidage of zeolite 5A pellets were proved that they were the important factors for simulation adsorption efficiency. CO_2 adsorption capacity increased with the decreasing temperature. The B0P2T5 without the binder gave the highest CO_2 adsorption capacity of 7.078 mmol CO_2/g under 200 kPa pressure and 5 min of compression time. The bentonite binder increased, interparticle voidage increased. Therefore, the gap between the zeolite particles was reduced and the attractive force between the zeolite surface and the CO_2 molecule was also reduced, resulting in a decreased adsorption capacity. Increased compression force at 400 kPa was resulted in zeolite particle size decreasing and getting a large BET surface area.

On the other hand, the mass transfer of B0P4T5 was low because the zeolite particles were too densely packed. The internal space may not be enough to allow the CO_2 molecules to move inside. Therefore, the CO_2 adsorption capacity was the lowest at a high compression force. The effect of compression time was the same as compression force. The compression time increased, mass transfer decreased. Moreover, simulation of industrial-scale CO_2 adsorption units in various situations with numerous beds, more complex cycles, and development of adsorbents, and additional research of the subroutines, have been planned for future development.

Acknowledgments

This work was supported in part by the faculty of engineering, King Mongkut's University of Technology North Bangkok (KMUTNB) No. ENG-62-62 and Center of Eco-Materials and Cleaner Technology

(CECT), Science and Technology Research Institute, King Mongkut's University of Technology North Bangkok. The author would like to thank Prof. Todsapon Thananatthanachon from the University of Evansville.

References

[1] L. Chen, T. Watanabe, H. Kanoh, K. Hata, and T. Ohba, "Cooperative CO_2 adsorption promotes high CO_2 adsorption density over wide optimal nanopore range," *Adsorption Science & Technology*, vol. 36, no. 1–2, pp. 625–639, 2017, doi: 10.1177/0263617417713573.

[2] P. A. P. Mendes, A. M. Ribeiro, K. Gleichmann, A. F. P. Ferreira, and A. E. Rodrigues, "Separation of CO_2/N_2 on binderless 5A zeolite," *Journal of CO_2 Utilization*, vol. 20, pp. 224–233, 2017, doi: 10.1016/j.jcou.2017.05.003.

[3] Q. H. Dirar and K. F. Loughlin, "Intrinsic adsorption properties of CO_2 on 5A and 13X zeolite," *Adsorption*, vol. 19, no. 6, pp. 1149–1163, 2013, doi: 10.1007/s10450-013-9543-2.

[4] M. Mofarahi and F. Gholipour, "Gas adsorption separation of CO_2/CH_4 system using zeolite 5A," *Microporous and Mesoporous Materials*, vol. 200, pp. 1–10, 2014, doi: 10.1016/j.micromeso.2014.08.022.

[5] A. I. Sarker, A. Aroonwilas, and A. Veawab "Equilibrium and kinetic behaviour of CO_2 adsorption onto zeolites, carbon molecular sieve and activated carbons," *Energy Procedia*, vol. 114, pp. 2450–2459, 2017, doi: 10.1016/j.egypro.2017.03.1394.

[6] K. Narang, K. Fodor, A. Kaiser, and F. Akhtar "Optimized cesium and potassium ion-exchanged zeolites A and X granules for biogas upgrading," *R S C Advances*, vol. 8, no. 65, pp. 37277–37285, 2018, doi: 10.1039/c8ra08004f.

[7] K. Narang and F. Akhtar, "Freeze granulated zeolites X and A for biogas upgrading," *Molecules*, vol. 25, no. 6, 2020, Art. no. 1378, doi: 10.3390/molecules25061378.

[8] L. Zhen, A. Carlos, D. Gran, L. Ping, Y. Jianguo, and E. R. Alirio, "Adsorption and desorption of carbon dioxide and nitrogen on zeolite 5A," *Separation Science and Technology*, vol. 46, no. 3, pp. 434–451, 2011, doi: 10.1080/01496395.2010.513360.

[9] A. Hyungwoong and M. Jong-Ho, "Diffusion mechanism of carbon dioxide in zeolite 4A and CaX pellets," *Adsorption*, vol. 10, no. 2, pp. 111–128, 2004.

[10] X. Xu, C. Song, R. Wincek, J. M. Andresen, B. G. Miller, and A.W. Scaroni, "Separation of CO_2 from power plant flue gas using a novel CO_2 "molecular basket" adsorbent," *Fuel Chemistry Division Preprints*, vol. 48, pp. 162–163, 2003.

[11] G. P. Knowles, P. A. Webley, Z. Liang, and A. L. Chaffee, *ACS Symposia*. Washington, DC: American Chemical Society, 2012, pp. 177–205.

[12] G. W. Peterson, J. B. Decoste, T. G. Glover, Y. Huang, H. Jasuja, and K. S. Walton, "Effects of pelletization pressure on the physical and chemical properties of the metal–organic frameworks $Cu_3(BTC)_2$ and UiO-66," *Microporous and Mesoporous Materials*, vol. 179, pp. 48–53, 2013.

[13] F. Rezaei, M. A. Sakwa-Novak, S. Bali, D. M. Duncanson, and C. W. Jones, "Shaping amine based solid CO_2 adsorbents: Effects of pelletization pressure on the physical and chemical properties" *Microporous and Mesoporous Materials*, vol. 204, pp. 34–42, 2015.

[14] U. S. P. R. Arachchige and M. C. Melaaen, "Aspen plus simulation of CO_2 removal from coal and gas fired power plants," *Energy Procedia*, vol. 23, pp. 391–399, 2012, doi: 10.1016/j.egypro.2012.06.060.

[15] A. Boonchuay, M. Srisawad, S. Sangsuradet, and P. Woratanakul, "Zeolite 13X and zeolite 5A as low-cost sustainable materials for cO_2 adsorption simulation," presented at the 8th International Conference on Green and Sustainable Innovation (ICGSI), Krabi, Thailand, Nov. 10–12, 2021.

[16] A. B. Hesam, H. Mohammad, and R. Niloofar, "Simulation of CH_4/CO_2 mixture separation by pressure swing adsorption in the Aspen Adsorption," presented at the 16th Iranian National Congress of Chemical Engineering, Tehran, Iran, Jan. 22, 2019.

[17] S. Sangsuradet, B. Wongchalerm, T. Arunchai, T. Khamkenbong, and P. Worathanakul, "Optimization of CO_2 adsorption and physical properties for pelletization of zeolite 5A," *Current Applied Science and Technology*, vol. 22, no. 3, pp. 1–11,

2022, doi: 10.55003/cast.2022.03.22.014
[18] Z. Liu, C. A. Grande, P. Li, J. Yu, and A. E. Rodrigues, "Adsorption and desorption of carbon dioxide and nitrogen on zeolite 5A," *Separation Science and Technology*, vol. 46, no. 3, pp. 434–451, 2011, doi: 10.1080/01496395.2010.513360.
[19] H. Thakkar, S. Eastman, A. Hajari, A. A. Rownaghi, J. C. Knox, and F. Rezaei, "3D-printed zeolite monoliths for CO_2 removal from enclosed environments," *ACS Applied Materials & Interfaces*, vol. 8, no. 41, pp. 27753–27761, 2016, doi: 10.1021/acsami.6b09647.
[20] K. Wood, Y. Liu, and Y. Yu. Design, *Simulation and Optimization of Adsorptive and Chromatographic Separations*. New York: John Wiley & Sons, 2018.
[21] C. Grande, "Advances in pressure swing adsorption for gas separation," *ISRN Chemical Engineering*, vol. 2012, 2012, Art. no. 982934, doi:10.5402/2012/982934.
[22] A. A. Norani, A. Ahmad, T. A. T. Abdullah, and A. Ripin, "Parametric study of CO_2 separation using carbon molecular sieve, zeolite and silica gel," *IOP Conference Series: Materials Science and Engineering*, vol. 808, 2020, Art. no. 012041, doi: 10.1088/1757-899x/808/1/012041.
[23] R. B. Bird, W. E. Stewart, and E. N. Lightfoot, *Transport Phenomena*. New York: Wiley, 1960, p. 511.
[24] D. D. Do, *Adsorption Analysis: Equilibria and Kinetics*. London: Imperial Coll Press, 1998.
[25] D. Stauffer and A. Aharony, *Introduction to Percolation Theory*. Boca Raton: CRC Press, 1994.
[26] F. G. Helfferich, *Principles of Adsorption & Adsorption Processes*. New York: John Wiley & Sons, 1985, pp. 523–524.
[27] F. M. Higgins, N. H. de Leeuw, and S. C. Parker, "Modelling the effect of water on cation exchange in zeolite A," *Journal of Materials Chemistry*, vol. 12, no. 1, pp. 124–131, 2001, doi: 10.1039/b104069n.
[28] J. Bedia, M. Peñas-Garzón, A. Gómez-Avilés, J. Rodriguez, and C. Belver, "A review on the synthesis and characterization of biomass-derived carbons for adsorption of emerging contaminants from water," *Journal of Carbon Research*, vol. 4, no. 4, 2018, Art. no. 63, doi: 10.3390/c4040063.
[29] P. S. Kumar, S. Ramalingam, C. Senthamarai, M. Niranjanaa, P. Vijayalakshmi, and S. Sivanesan, "Adsorption of dye from aqueous solution by cashew nut shell: Studies on equilibrium isotherm, kinetics and thermodynamics of interactions," *Desalination*, vol. 261, no. 1–2, pp. 52–60, 2010, doi: 10.1016/j.desal.2010.05.032.
[30] M. Sekar, V. Sakthi, and S. Rengaraj, "Kinetics and equilibrium adsorption study of lead(II) onto activated carbon prepared from coconut shell," *Journal of Colloid and Interface Science*, vol. 279, no. 2, pp. 307–313, 2004, doi: 10.1016/j.jcis.2004.06.042.
[31] J. C. Moreno-Piraján and L. Giraldo, "Activated carbon obtained by pyrolysis of potato peel for the removal of heavy metal copper (II) from aqueous solutions," *Journal of Analytical and Applied Pyrolysis*, vol. 90, no. 1, pp. 42–47, 2011, doi: 10.1016/j.jaap.2010.10.004.
[32] C. Garnier, G. Finqueneisel, T. Zimny, Z. Pokryszka, S. Lafortune, P. D. C. Défossez, and E. C. Gaucher, "Selection of coals of different maturities for CO_2 Storage by modelling of CH_4 and CO_2 adsorption isotherms," *International Journal of Coal Geology*, vol. 87, no. 2, pp. 80–86, 2011, doi: 10.1016/j.coal.2011.05.00.
[33] J. M. Martín-Martínez, "Adsorción física de gases y vapores por carbones," Universidad de Alicante, Alicante, Spain, 1990.
[34] A. Charkh7i, M. Kazemeini, S. J. Ahmadi, and H. Kazemian, "Fabrication of granulated NaY zeolite nanoparticles using a new method and study the adsorption properties," *Powder Technology*, vol. 231, pp. 1–6, 2012, doi: 10.1016/j.powtec.2012.06.041.
[35] S. Budsaereechai, K. Kamwialisak, and Y. Ngernyen, "Adsorption of lead, cadmium and copper on natural and acid activated bentonite clay," *Asia-Pacific Journal of Science and Technology*, vol. 17, no. 5, pp. 800–810, 2012.
[36] M. Puccini, E. Stefanelli, M. Seggiani, and S. Vitolo, "Removal of CO_2 from flue gas at high temperature using novel porous solids," *Chemical Engineering Transactions*, vol. 47, pp. 139–144, 2016.
[37] H. Thakkar, S. Eastman, A. Hajari, A. A. Rownaghi, J. C. Knox, and F. Rezaei, "3D-printed zeolite monoliths for CO_2 removal from

enclosed environments," *ACS Applied Materials & Interfaces*, vol. 8, no. 41, pp. 27753–27761, 2016, doi: 10.1021/acsami.6b09647.

[38] K. Sepsirisuk, P. Vittaya, and T. Nipon. "Comparative studies on adsorption capacity of phorbol esters in Jatropha curcas seed oil with different type of bentonites," presented at the 47th Kasetsart University Annual Conference, Bangkok, Thailand, Mar. 17–20, 2009.

[39] F. Rezaei, M. A. Sakwa-Novak, S. Bali, D. M. Duncanson, and C. W. Jones, "Shaping aminebased solid CO_2 adsorbents: Effects of pelletization pressure on the physical and chemical properties," *Microporous and Mesoporous Materials*, vol. 204, pp. 34–42, 2014, doi: 10.1016/j.micromeso.2014.10.047.

[40] C. Chen, D. W. Park, and W. S. Ahn, "Surface modification of a low-cost bentonite for post-combustion CO_2 capture," *Applied Surface Science*, vol. 283, pp. 699–704, 2013.

[41] E. Vilarrasa-García, J. A. Cecilia, D. C. S. Azevedo, C. L. Cavalcante, and E. Rodríguez-Castellón, "Evaluation of porous clay heterostructures modified with amine species as adsorbent for the CO_2 capture," *Microporous Mesoporous Mater*, vol. 249, pp. 25–33, 2017.

[42] G. Gómez-Pozuelo, E. S. Sanz-Pérez, A. Arencibia, P. Pizarro, R. Sanz, and D. P. Serrano, "CO_2 adsorption on amine-functionalized clays," *Microporous Mesoporous Mater*, vol. 282, pp. 38–47, 2019.

[43] H. Wang, Z. G. Qu, J. Q. Bai, and Y. S. Qiu, "Combined grand canonical Monte Carlo and finite volume method simulation method for investigation of direct air capture of low concentration CO_2 by 5A zeolite adsorbent bed," *International Journal of Heat and Mass Transfer*, vol. 126, pp. 1219–1235, 2018, doi: 10.1016/j.ijheatmasstransfer.2018.06.052.

[44] M. Puccini, E. Stefanelli, M. Seggiani, and S. Vitolo, "Removal of CO_2 from flue gas at high temperature using novel porous solids," *Chemical Engineering Transactions*, vol. 47, pp. 139–144, 2016.

[45] F. A. A. Kareem, A. M. Shariff, S. Ullah, F. Dreisbach, L. K. Keong, N. Mellon, and S. Garg, "Experimental measurements and modeling of supercritical CO_2 adsorption on 13X and 5A zeolites," *Journal of Natural Gas Science and Engineering*, vol. 50, pp. 115–127, 2018, doi: 10.1016/j.jngse.2017.11.016.

[46] Z. Liu, C. A. Grande, P. Li, J. Yu, and A. E. Rodrigues, "Adsorption and desorption of carbon dioxide and nitrogen on zeolite 5A," *Separation Science and Technology*, vol. 46, no. 3, pp. 434–451, 2011, doi: 10.1080/01496395.2010.51336.